Interlayer Energy Transfer between Carbazole and Two 9-Anthroyloxy Derivatives in Langmuir−Blodgett Films

Kristine Kilså Jensen,[†] Bo Albinsson,[†] Mark Van der Auweraer,[‡] Elina Vuorimaa,*[,§] and Helge Lemmetyinen[§]

Department of Physical Chemistry, Chalmers University of Technology, SE-412 96 Göteborg, Sweden; Laboratories for Molecular Dynamics and Spectroscopy, Chemistry Department, K. U. Leuven, Celestijnenlaan 200 F 3001, Leuven, Belgium; and Institute of Materials Chemistry, Tampere University of Technology, P.O. Box 541, FIN-33101 Tampere, Finland

Received: February 24, 1999; In Final Form: July 6, 1999

The interlayer excitation energy transfer between 11-(9-carbazole)undecanoic acid (11-CU) and two 9-anthroyloxy derivatives, 9-(9-anthroyloxy)stearic acid (9-AS) and 2-(9-anthroyloxy)stearic acid (2-AS), in alternating multilayer Langmuir−Blodgett films has been studied. The 11-CU fluorescence is quenched by energy transfer to 9-AS or 2-AS as judged by steady-state and picosecond time-resolved fluorescence measurements. The fluorescence decay curves of 11-CU in the films were analyzed in the framework of several models: (1) a general model for interlayer energy transfer, (2) a two-exponential decay, (3) a Förster model for energy transfer in a two-dimensional system, and (4) a stretched-exponential decay, characteristic of Förster energy transfer in self-similar fractal-like structures. The recovered decay parameters suggest an inhomogeneous mixing of the acceptor molecules in LB films leading to a two-phase system. The phase separation during compression of the acceptor monolayers forms regions of acceptor concentration about 3 times that of the intended and regions with very low acceptor concentration.

1. Introduction

Special attention has recently been focused on the dynamics of energy transfer and relaxation in restricted molecular geometries such as Langmuir−Blodgett (LB) films.[1−7] The LB technique is suitable for studying energy transfer for the following reasons: (i) the monolayer thickness can be precisely controlled yielding a well-defined donor/acceptor distance distribution, (ii) multilayer structures with varying layer composition can be made, and (iii) molecules can selectively be oriented in the film. The high degree of orientation of molecules in LB films can cause a configurational and dynamic behavior quite different from that obtained in a homogeneous solution. Understanding the relationship between the mechanism of excitation energy transfer and the distribution and orientation of chromophores in a two-dimensional plane is essential for the construction of functional molecular assemblies.

In the present study the interlayer excitation energy transfer between a carbazole derivative, 11-(9-carbazole)undecanoic acid (11-CU), and two 9-anthroyloxy derivatives in LB films has been examined. The distance between the donor 11-CU and the acceptor was varied by using two different 9-anthroyloxy derivatives: 9-(9-anthroyloxy)stearic acid (9-AS) and 2-(9-anthroyloxy)stearic acid (2-AS). Efficient energy transfer can be expected between the donor and acceptor molecules in view of the large overlap between the emission spectrum of 11-CU and the absorption spectra of the 9-anthroyloxy derivatives.

The observed nonexponential fluorescence decay curves were analyzed in the framework of four models: (1) a model for interlayer energy transfer proposed by Baumann and Fayer[8] (BF model), (2) the limit of the BF model where the layers are far apart, giving an exponential model (EXP-model), (3) the limit of the BF model where donors and acceptors are in the same layer, giving a Förster model for energy transfer in a two-dimensional system[8,9] (2DF model), and (4) a stretched-exponential model, characteristic of Förster energy transfer in self-similar fractal-like structures (SE model).[9]

2. Experimental Section

Water was purified by a Milli-RO/Milli-Q system (Millipore). Chloroform, toluene (J. T. Baker), 11-CU, 9-AS, 2-AS (Molecular Probes), and stearylamine (SA) (Aldrich) were used without further purification. The structures of the modified fatty acids are shown in Figure 1.

The critical Förster distance for the donor/acceptor pairs was determined in 5 μM toluene solutions. Absorption spectra were recorded on a Shimadzu UV-2501PC spectrophotometer, and steady-state fluorescence emission spectra were obtained with a SPEX Fluorolog 3 spectrofluorometer.

LB films were prepared with a KSV 5000 alternate LB system (KSV Instruments). Aqueous 0.6 mM phosphate buffer (pH = 7.0) was used as a subphase. The temperature of the subphase was 18.5 ± 0.5 °C. The films were deposited on quartz plates cleaned with sulfochromic acid and plasma etched with nitrogen just before use with a PDC-23G (Harrick) plasma cleaner. Nitrogen pressure was about 0.15 mbar, and the plates were etched for 15 min. Mixtures of the modified fatty acids and SA were spread on the subphase from chloroform solutions. The mixed monolayers were compressed at a rate of 0.53 Å^2 molecule^{-1} min^{-1}. For the pure chromophore monolayers the compression rate was 0.36 Å^2 molecule^{-1} min^{-1}. The films were

[†] Chalmers University of Technology.
[‡] K. U. Leuven.
[§] Tampere University of Technology.
* To whom correspondence should be addressed.

10.1021/jp990666j CCC: $18.00
Published on Web 09/16/1999

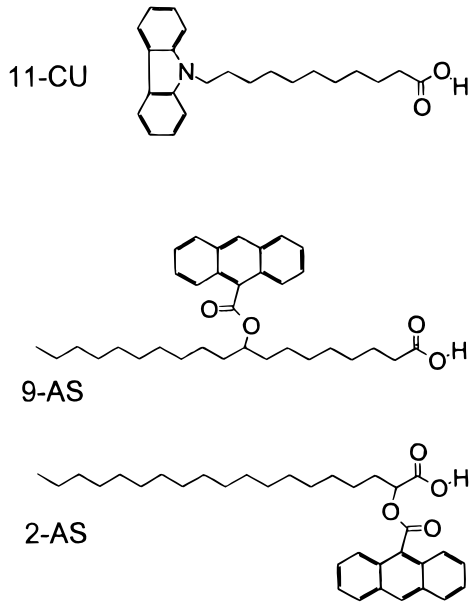

Figure 1. Structures of 11-(9-carbazole)undecanoic acid (11-CU), 9-(9-anthroyloxy)stearic acid (9-AS), and 2-(9-anthroyloxy)stearic acid (2-AS).

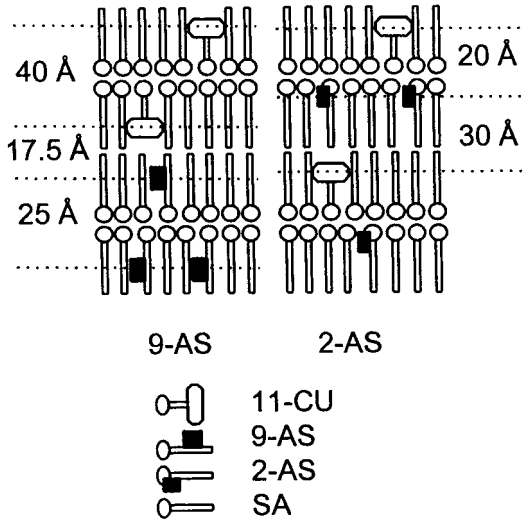

Figure 2. Schematic representation of the LB films and the estimated[10] minimum interlayer chromophore−chromophore distances.

deposited at 20 mN m^{-1}, and the dipping rates were 10 mm min^{-1} upward and 20 mm min^{-1} downward. Slow movement of the substrate through the film during dipping is recommended for good quality films. However, in downward deposition, too slow a dipping rate often leads to the peeling off of the last layer rather than to the deposition of a new layer. Thus, according to our experience with various chromophore/matrix systems using higher deposition speed for downward deposition than for upward deposition yields better quality films. The quartz plates were precoated with nine SA bottom layers.

Two different multilayer systems were constructed (Figure 2). In both systems 20 11-CU containing and 20 9-AS or 2-AS containing layers were deposited on both sides of the quartz plates. The layers are in a tail-to-tail configuration, and interlayer dimer formation or aggregation was therefore avoided. For spectroscopic measurements the concentration of 11-CU was 1 mol %, and the acceptor concentration varied between 0 and 5 mol %. To study interlayer energy transfer between 11-CU and 9-AS, a double alternating deposition of 11-CU containing monolayers and 9-AS containing monolayers in SA matrix was made. The minimum distance between 11-CU and 9-AS was estimated to be 17.5 Å.[10] In the other system an alternating deposition of monolayers containing 11-CU or 2-AS in SA matrix was made. In this system the minimum distance between 11-CU and 2-AS was estimated to be 20 Å.[10]

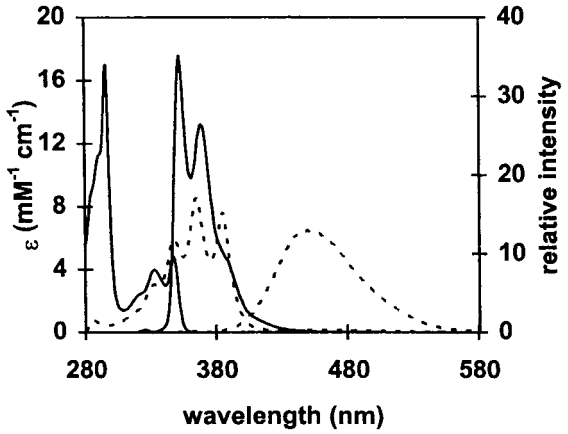

Figure 3. Absorption and emission spectra of 11-CU (—) and 2-AS (- - -) in toluene. The excitation wavelength was 325 nm.

The steady-state fluorescence emission from the LB films was measured by aligning the quartz plates at an angle of 60° with respect to the direction of the excitation beam. The emission was detected in a 90° configuration from the backside of the quartz plate to avoid reflections. The fluorescence decay curves were measured with a time-correlated single-photon-counting system (Edinburgh Instrument 199) as described previously.[5] The samples were excited by 10 ps pulses at the wavelength of 295 nm, and the response time of the instrument setup was about 120 ps (fwhm). The fluorescence was observed through a Glan-Thompson polarizer set at the magic angle.

The fluorescence decays were analyzed, either as single curves or globally, by iterative reconvolution using a Marquardt algorithm.[11−13] The quality of the fit was judged in terms of the statistical parameters χ^2 and χ^2_g (for an acceptable fit less than 1.30 and 1.20, respectively) and Z_{χ^2}, the runs test,[14] and the Durbin−Watson parameters[15] and by visual inspection of the weighted residuals and their autocorrelation function.[16] To reduce the number of adjustable parameters, leading to a better model discrimination and more accurate recovery of the parameters,[17,18] decays obtained for different concentrations of the energy acceptor were analyzed globally linking τ_D and τ_2 in the 2DF model or linking τ_D, R_0/d, and τ_2 in the BF model. To correct for scattered light and digitization errors, $B\delta(t)$, where B is the scatter parameter, is added to the different expressions for the decays discussed earlier. In the analyses the preexponential factor $I(0)$ was always much larger than the scatter parameter B, suggesting that the function $B\delta(t)$ does not hide a fast decaying component.

3. Results

Measurements in Solution. The absorption and fluorescence spectra of 11-CU and 2-AS in toluene are shown in Figure 3. In contrast to unsubstituted anthracene, broad structureless emission bands, characteristic of the anthroyloxy chromophores, are observed for 2-AS and 9-AS.[19]

In the Förster theory for energy transfer[20] the critical distance, R_0, is the distance between donor and acceptor at which the rate constant for energy transfer is equal to the sum of rate constants for all other deactivation processes of the donor. The critical distance can be calculated from photophysical properties

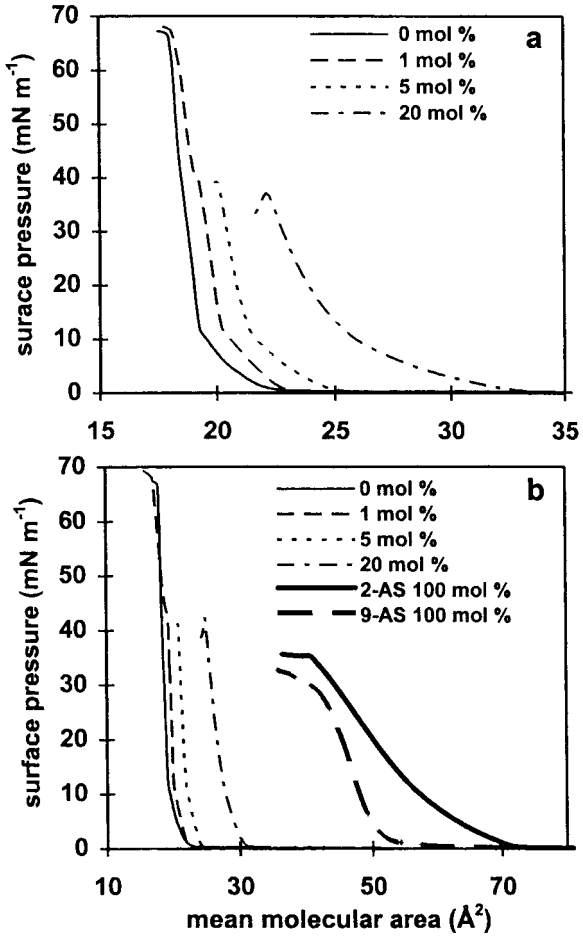

Figure 4. Surface pressure−area isotherms for (a) mixed films of 11-CU and SA (b) mixed films of 2-AS and SA and pure 2-AS and 9-AS. Concentrations are marked in the figure. At low concentrations from 1 to 20 mol % the isotherms of 2-AS and 9-AS are identical.

of the separate donor and acceptor moieties

$$R_0^6 = \frac{9000(\ln 10)}{128\pi^5 N_A}\frac{\kappa^2\phi_D}{n^4}\int_0^\infty F_D(\lambda)\,\epsilon_A(\lambda)\lambda^4\,d\lambda \qquad (1)$$

where N_A is the Avogadro number, $n = 1.5$ is the solvent refractive index,[21] and κ^2 is an orientation factor that depends on the relative orientation of the transition dipoles involved in the donor fluorescence and acceptor absorption. The dynamic average value for isotropic systems $\kappa^2 = {}^2/_3$ was used.[22] The fluorescence quantum yield of the donor in the absence of energy transfer was determined to be $\phi_D = 0.5$ in diluted toluene solution at 25 °C. Anthracene ($\phi = 0.29$ in toluene[23]) was used as a reference. The spectral overlap of the donor fluorescence band $F_D(\lambda)$ (normalized to unity) with the absorption spectrum $\epsilon_A(\lambda)$ of the acceptor was calculated to be 9.5×10^{-15} M^{-1} cm^{-3}. Thus, $R_0 = 28$ Å was obtained for the carbazole/9-anthroyloxy pairs. This value is in good agreement with the literature value of 27.7 Å for the carbazole/anthracene pair.[24]

Film Properties. The pressure−area isotherms obtained for mixed monolayers of the chromophores and SA are shown in Figure 4. No pressure−area isotherm characteristic for a condensed phase was observed for 100 mol % 11-CU film on the subphase used, although it has been observed on a 0.3 mM $CdCl_2$ subphase.[25] The collapse pressure of the mixed films increases from 37 mN m^{-1} for 20 mol % film to 67 mN m^{-1} for 1 mol % film. The slope change observed for the 1 mol % film around 40 mM m^{-1} indicates the exclusion of 11-CU from the film of SA leading to an inhomogeneous film at higher pressures. This kind of behavior is often observed for mixed films.[26,27]

TABLE 1: Mean Molecular Areas (MMA) and Number Densities (σ_i = Molar Fraction of the Chromophore/Mean Molecular Area of the Film) of 2-AS, 9-AS, and 11-CU in LB Films at the Deposition Pressure of 20 mN m^{-1}

film	MMA (nm^2)	σ_i (nm^{-2})
1 mol % 11-CU, 9-AS and 2-AS	0.196	0.051
2 mol % 9-AS and 2-AS	0.200	0.100
3 mol % 9-AS and 2-AS	0.203	0.148
5 mol % 9-AS and 2-AS	0.208	0.240

The 100 mol % 2-AS and 9-AS monolayers show a smooth rise in the surface pressure characteristic for a liquid-expanded phase and a clear collapse point at 36 mN m^{-1} (Figure 4b). The behavior of 2-AS is in agreement with the isotherms observed for $CdCl_2$ subphase.[28] For a pure 9-AS film the initial increase of the surface pressure takes place at much lower molecular areas than for 2-AS, although at the collapse point the molecular areas are nearly identical for both substances. Similar behavior has been observed for corresponding *n*-(9-anthroyl)fatty acids.[29] The behavior of the monolayers of the two anthroyloxy chromophores mixed with SA is identical and similar to the behavior of 11-CU mixed with SA. The collapse pressure of the mixed films is 42 mN m^{-1} for chromophore concentrations between 2 and 20 mol %. For the 1 mol % film, a slope change around 42 mM m^{-1} is observed, and the collapse takes place at 67 mM m^{-1}.

From the mean molecular areas, the surface densities σ_i (number of molecules per unit area) of the modified fatty acids at the deposition pressure can be calculated (Table 1).

Interlayer Energy Transfer. The fluorescence spectra of the LB films with different acceptor concentrations excited at 295 nm are shown in Figure 5. The fluorescence intensity of 11-CU at 350 nm decreases and the fluorescence intensities of 2-AS and 9-AS at 440 nm increase with increasing concentration of the acceptors, indicating that interlayer excitation energy transfer occurs from 11-CU to 2-AS and 9-AS. Using 295 nm as the excitation wavelength, the fluorescence of the 9-anthroyloxy chromophores in the absence of 11-CU is very weak. The fluorescence spectra of 1 mol % anthroyloxy films shown in Figure 5 have been multiplied by a factor of 10.

The fluorescence decay curves of 11-CU obtained at different acceptor concentrations are shown in Figure 6. The quenching of 11-CU fluorescence is observed as an increase of the fluorescence decay rate and deviation from the exponential behavior. In the absence of acceptors a fluorescence lifetime of 10.8 ± 0.2 ns was obtained by one-exponential analysis of the decay curves. This is in agreement with the fluorescence lifetime obtained in dilute toluene solution ($\tau_D = 11.0 \pm 0.2$ ns). In the four models used to analyze the donor fluorescence decay curves, the fluorescence lifetime of the donor in the absence of acceptors, τ_D, was fixed at 10.8 ns.

Since the distribution of the acceptors in the films is unknown, the models are divided into three submodels according to the assumed distribution of the acceptors: (1) homogeneous distribution of acceptors; (2) the acceptor layers having two phases, one containing only SA and the other containing SA and acceptor molecules; and (3) the acceptor layers having two phases, one of high acceptor concentration and the other of low acceptor concentration. If upon increasing the acceptor concentration the fraction of the layer occupied by the high acceptor concentration phase increases, the concentration of the acceptor containing phases should stay approximately constant.

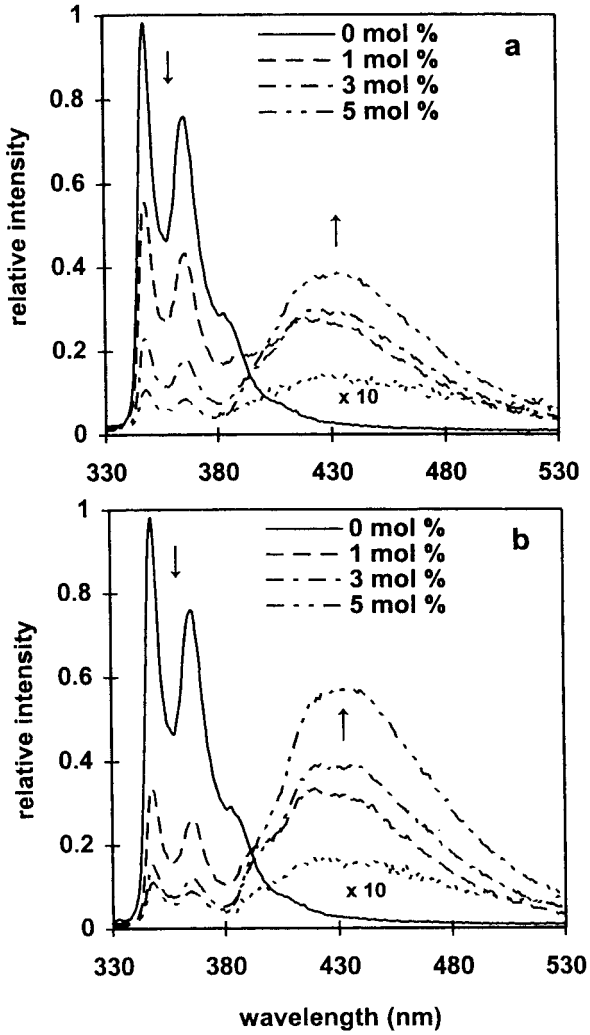

Figure 5. Fluorescence spectra of 1 mol % 11-CU films with 0, 1, 3, and 5 mol % (a) 2-AS and (b) 9-AS. Concentrations are marked in the figure. For comparison, the fluorescence spectra of 1 mol % 9-AS and 2-AS, multiplied by a factor of 10, in the absence of 11-CU are shown (· · ·). The excitation wavelength was 295 nm.

BF Model. Baumann and Fayer[8] derived the theoretical expressions for electronic excitation energy transfer in multilayered structures containing donors and acceptors under various conditions of interlayer distance, density of molecules, number of stacking layers, and orientational distributions of molecules. The probability of the excitation energy appearing on the initially excited molecules, $G(t)$, can be probed by the fluorescence from the donor molecules and is determined by the surface density of acceptors σ_i, the ratio of the chromophore layer separation (d), and the Förster radius (R_0). If the two layers are far apart compared with R_0, $G(t)$ decays exponentially. In the limit where the layers are infinitely close, the BF model transforms into the 2-dimensional Förster model. When the ratio R_0/d is close to unity, $G(t)$ is most sensitive to the variation of the layer separation. In this case the decay curves of the donor can be described as

$$I(t) = c_1 \exp[-t/\tau_D]G(t) \tag{2}$$

where c_1 is an instrumental factor and t is the time in nanoseconds. For interlayer energy transfer and isotropic orientation of the chromophore dipoles $G(t)$ is expressed as[8]

$$\ln[G(\mu)] = \sigma_i \pi d^2[1 - \exp(-\mu\langle\kappa^2\rangle) - (\mu\langle\kappa^2\rangle)^{1/3}\gamma(^2/_3,\mu\langle\kappa^2\rangle)] \tag{3}$$

where

$$\mu = \frac{3}{2}\frac{t}{\tau_D}\left(\frac{R_0}{d}\right)^6 \tag{4}$$

and

$$\gamma(^2/_3,l) = \int_0^l \exp[-s]s^{-1/3}\mathrm{d}s \tag{5}$$

is the incomplete γ function. s is a dummy variable, and γ is a dimensionless parameter defining the dimensionality of the quenching. It governs the transition from an exponential behavior at short times or small R_0/d to a stretched exponential behavior characteristic for in-plane energy transfer for long times or large R_0/d.

The decay curves were simulated with this model, since in principle all the parameters are known. For R_0 the value of 28 Å obtained from solution measurements and for $\langle\kappa^2\rangle$ the isotropic average value of $^2/_3$ were used. The surface densities of the acceptor molecules, σ_i, were obtained from the pressure−area isotherms (Table 1), and as donor−acceptor layer distances the estimated values of 17.5 and 20 Å for 9-AS and 2-AS films, respectively, were used (Figure 2). The fluorescence decay curves obtained for films at different acceptor concentrations

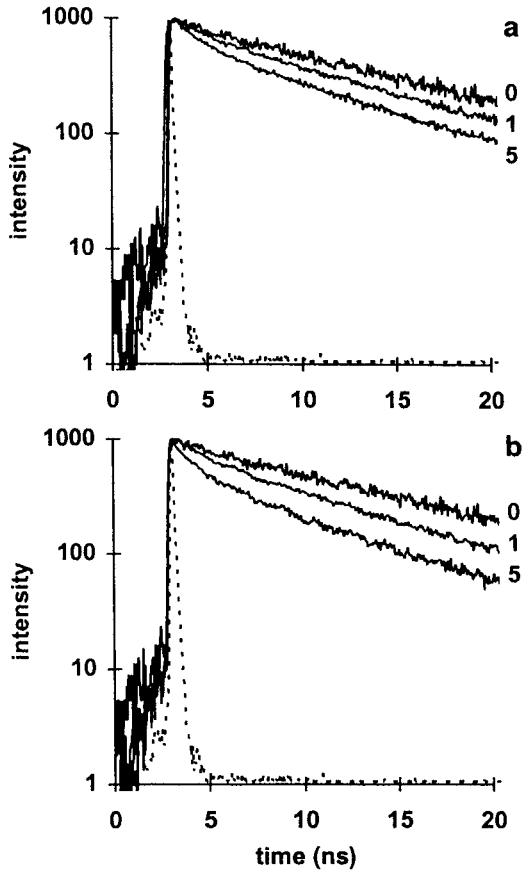

Figure 6. Fluorescence decay curves of 1 mol % 11-CU films with 0, 1, and 5 mol % of (a) 2-AS and (b) 9-AS together with (4) the instrumental response function (· · ·). Concentrations are marked in the figure. The excitation wavelength was 295 nm, and the fluorescence decay curves were monitored at 350 nm.

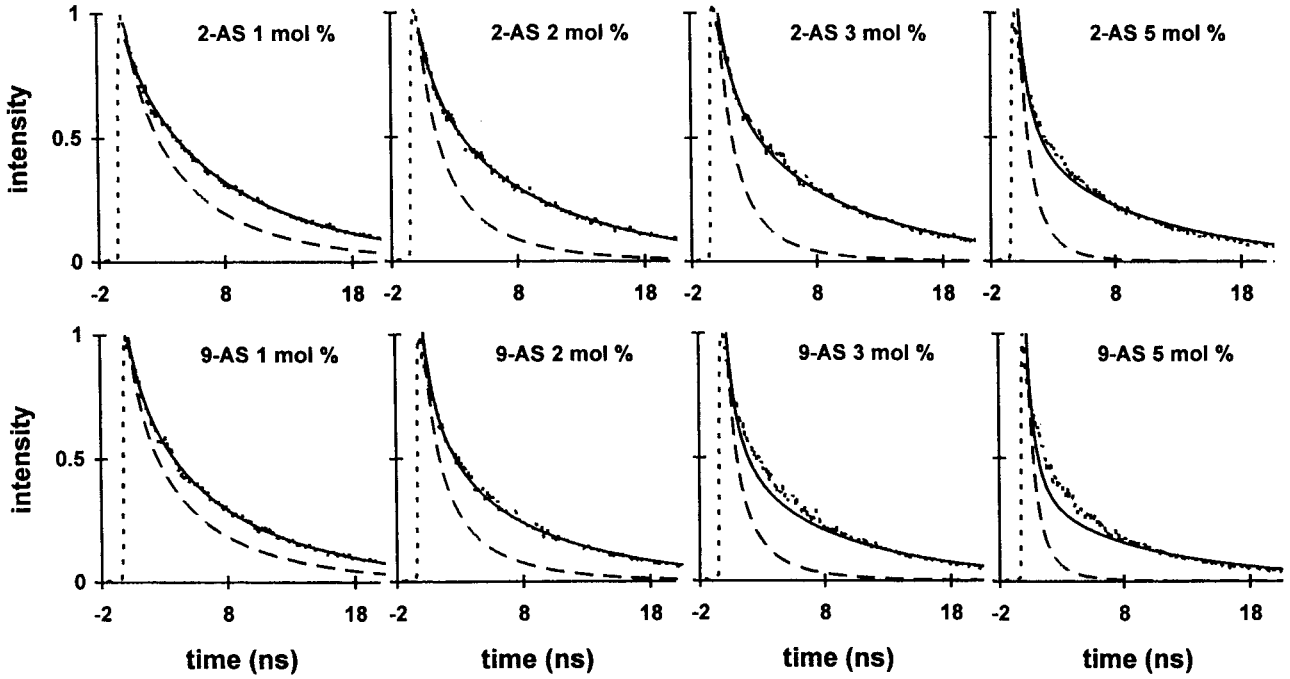

Figure 7. Fluorescence decay curves (· · ·) of 1 mol % 11-CU films with different concentrations (marked in the figure) of 2-AS and 9-AS together with the simulated data according to the BF model without (- - -) and with (—) the extra exponential term. The excitation wavelength was 295 nm, and the fluorescence decay curves were monitored at 350 nm.

are shown in Figure 7 together with the simulated decay curves. The simulated decays are clearly far too fast compared with the observed decays.

When the fluorescence decays of other chromophores in other multilayers[30,31] have been analyzed in the framework of the submodels 2 and 3, including an additional exponentially decaying component in the decay was always necessary. The interpretation of this extra term is different in the two submodels. While in the submodel 2 the extra term should be attributed to the presence of donor molecules not affected by any acceptors; in the framework of submodel 3 the extra component is attributed to donors contacting a phase with high acceptor concentration. Thus, in submodel 2 τ_D and τ_2 should coincide, but in submodel 3 they should differ strongly in the framework of our interpretation. In the case of inhomogeneous acceptor distribution the equation for interlayer energy transfer becomes

$$I(t) = C[(1 - \alpha)\exp(-t/\tau_D)G(t) + \alpha\exp(-t/\tau_2)] \quad (6)$$

where C is an instrumental factor. In submodel 2, $1 - \alpha$ corresponds to the fraction of donors contacting an acceptor containing phase, while α corresponds to the fraction of donors not contacting an acceptor containing phase. In submodel 3, $1 - \alpha$ corresponds to the fraction of donors contacting a phase of small acceptor concentration, while α corresponds to the fraction of donors contacting a phase of a very high acceptor concentration.

BF Model, Submodel 2. For submodel 2 (BF2), the donor fluorescence decay curves were simulated with eq 6, fixing τ_2 at 10.8 ns and allowing the parameters c_1 and c_2 to vary. Including the exponentially decaying term in the simulations gives a better agreement with the measured decay curves (Figure 7), but the analysis still fails at high acceptor concentrations: for 2-AS the model fails at 5 mol % concentration, whereas for 9-AS it fails already at 3 mol % concentration. The normalized, relative proportions of "energy transfer donors", α, and "free donors", $1 - \alpha$, do not change significantly with the acceptor concentrations between 1 and 3 mol %: $1 - \alpha$ being 0.53 and 0.35 for 2-AS and 9-AS films, respectively. With an acceptor concentration of 5 mol % $1 - \alpha$ changes to 0.39 and 0.23 for 2-AS and 9-AS films, respectively.

For an inhomogeneous distribution of acceptors the local acceptor concentration is no longer constant for all donors. In the BF2 simulations, surface densities of the acceptor molecules obtained from the pressure—area isotherms were used. However, in the case of an inhomogeneous distribution of acceptors, the local surface density of acceptors will be larger (submodel 2) or smaller (submodel 3) than the overall surface density of acceptors. Therefore, the decays were fitted to eq 6, which allowed the recover of the parameters R_0/d, c_1, c_2, and $\gamma_{IL} = b\sigma_i\pi R_0^2(\tau_D)^{-1/3}$. The equation for γ_{IL} comes from the assumption that both the donor and acceptor molecules reside in the same monolayer or that their average distance is dominated by the component in the plane of the film. In this case the energy transfer becomes essentially two-dimensional. The parameter b is related to the number of anthroyloxy layers contacting the 11-CU layer, being 1 for systems with acceptor layers on both sides of the donor layer and 0.5 for systems with an acceptor layer only on one side of the donor layer (Figure 2). Global analysis with τ_2 fixed at 10.8 ns resulted in acceptable statistical fits (Table 2). Now the fraction of "free donors" decreases upon increasing acceptor concentration. Comparing the obtained R_0/d values with the estimated distances shown in Figure 2, the value of 1.9 ± 0.3 obtained for 2-AS is reasonable, yielding $d = 28$ Å$/1.9 = 14.7$ Å, but the value of 5.2 ± 3.2 obtained for 9-AS yielding $d = 28$ Å$/5.2 = 5.4$ Å is still unreasonable. This can be due to parameter correlation, and thus the R_0/d values were fixed to the estimated values of 1.6 and 1.4 Å for 9-AS and 2-AS, respectively. For 9-AS good statistical parameters (Table 2) were obtained, but for 2-AS the fit failed. The obtained γ_{IL} values increase linearly with increasing acceptor concentration but do not approach zero at low acceptor concentrations for either system (Figure 8). The latter would be expected as in the absence of quencher, the decay should become single-exponential with a decay time equal to τ_D.

TABLE 2: Parameters Obtained by Global Analysis of the Donor Fluorescence Decay Curves in the Framework of Eq 6 with the Exponentially Decaying Term Fixed at 10.8 (BF2) and Free (BF3)[a]

model global parameters	[*i*-AS] (mol %)	2-AS γ_{IL}	2-AS $1-\alpha$	2-AS χ^2	model global parameters	9-AS γ_{IL}	9-AS $1-\alpha$	9-AS χ^2
BF2					BF2			
$R_0/d = 1.9 \pm 0.3$	0			1.20	$R_0/d = 5.2 \pm 3.2$			1.20
$\chi_g^2 = 1.14$	1	0.50	0.50	1.10	$\chi_g^2 = 1.14$	0.18	0.35	1.10
	2	0.51	0.43	1.11		0.19	0.28	1.15
	3	0.54	0.39	1.19		0.21	0.20	1.13
	5	0.59	0.29	1.11		0.24	0.19	1.16
R0/d = 1.4 fixed	0			1.18	R0/d = 1.6 fixed			1.18
$\chi_g^2 = 1.26$	1	0.78	0.57	1.14	$\chi_g^2 = 1.16$	0.45	0.36	1.12
	2	0.78	0.50	1.28		0.47	0.29	1.14
	3	0.82	0.46	1.36		0.51	0.22	1.15
	5	0.88	0.36	1.33		0.60	0.21	1.21
BF3					BF3			
$R_0/d = 1.7 \pm 1.7$	0			1.20	$R_0/d = 1.4 \pm 3.3$			1.20
$\tau_2 = 1.2 \pm 0.5$ ns	1	0.07	0.23	1.11	$\tau_2 = 1.0 \pm 0.7$ ns	0.15	0.24	1.10
$\chi_g^2 = 1.16$	2	0.09	0.26	1.15	$\chi_g^2 = 1.15$	0.18	0.27	1.15
	3	0.10	0.29	1.20		0.23	0.30	1.15
	5	0.13	0.35	1.13		0.24	0.38	1.13
$R_0/d = 1.4$ fixed	0			1.20	$R_0/d = 1.6$ fixed			1.20
$\tau_2 = 1.2 \pm 0.2$ ns	1	0.07	0.25	1.10	$\tau_2 = 1.0 \pm 0.2$ ns	0.14	0.19	1.10
$\chi_g^2 = 1.16$	2	0.09	0.29	1.13	$\chi_g^2 = 1.13$	0.18	0.22	1.08
	3	0.10	0.32	1.20		0.22	0.24	1.15
	5	0.14	0.39	1.16		0.22	0.32	1.13

[a] τ_D is fixed at 10.8 ns.

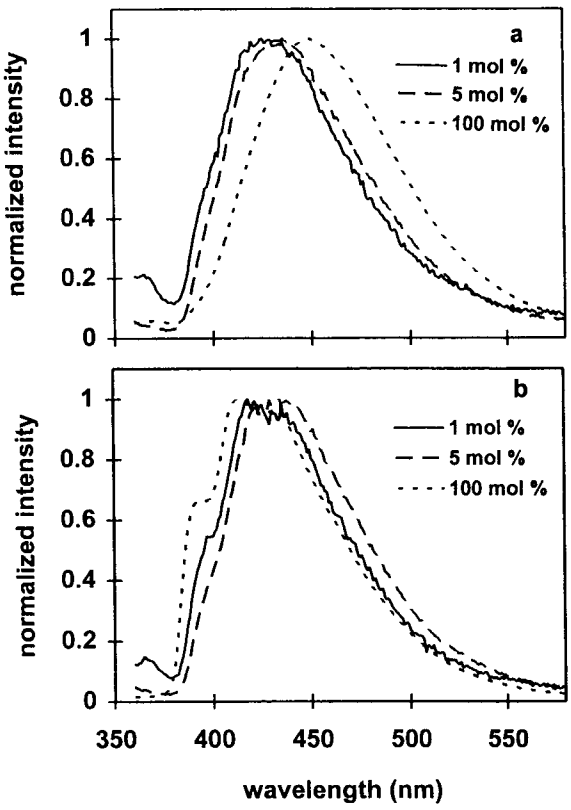

Figure 8. Normalized fluorescence spectra of 1, 5, and 100 mol % films of (a) 2-AS and (b) 9-AS. Concentrations are marked in the figure. The excitation wavelength was 330 nm.

BF Model, Submodel 3. To consider the second case of acceptor distribution, i.e., the acceptor layers have two phases, one of high acceptor concentration and the other of low acceptor concentration (submodel 3), the decay curves were fitted with eq 6 without fixing the lifetime of the exponentially decaying term (BF3 model). Now the exponential term corresponds to the decay of 11-CU molecules contacting a phase of the acceptor layer with a high acceptor concentration. Again global analysis

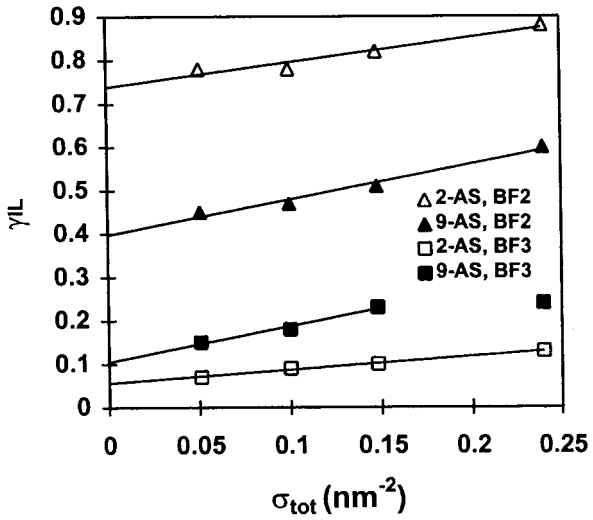

Figure 9. Plot of γ_{IL} obtained from models BF2 and BF3 (R_0/d fixed) as a function of the total number density of acceptors.

resulted in acceptable statistical fits (Table 2). The fluorescence lifetimes τ_2 of 1.2 and 1.0 ns for the 2-AS/11-CU and the 9-AS/11-CU system were obtained. The R_0/d values have very large error values for both acceptors, and thus the R_0/d values were fixed to the estimated values. Good statistical parameters and nearly identical results as when allowing R_0/d to float (Table 2) were obtained. The γ_{IL} values are much smaller than those obtained with the BF2 model, suggesting a significantly lower surface density of acceptors. For 2-AS the obtained γ_{IL} values increase linearly with increasing acceptor concentration, but for 9-AS the linear dependence breaks down at 5 mol % concentration (Figure 8, model BF3).

EXP Model. In the limit where the donor and acceptor layers are far apart compared with R_0, $G(t)$ decays exponentially, and the decay constant depends on the specific conditions such as R_0/d, τ_D, and σ_i. The observed fluorescence decay curves cannot be fitted to a one-exponential decay (EXP1-model). Thus, taking into account the extra exponentially decaying component due to an inhomogeneous distribution of acceptors, the expression

TABLE 3: Parameters Obtained by Two-Exponential Analysis of the Donor Fluorescence Decays in the Presence of 2-AS and 9-AS

model *i*-AS	[*i*-AS] (mol %)	τ_2 (ns)	τ_1 (ns)	$1-\alpha$	χ^2
EXP2					
2-AS	1	2.4	10.8	0.37	1.32
	2	2.3	10.8	0.44	1.29
	3	2.4	10.8	0.46	1.59
	5	2.3	10.8	0.57	2.46
9-AS	1	3.1	10.8	0.49	1.82
	2	2.9	10.8	0.58	2.34
	3	3.1	10.8	0.64	2.03
	5	2.5	10.8	0.71	2.67
EXP3					
2-AS	1	1.8	10.1	0.32	1.16
	2	1.9	10.1	0.39	1.10
	3	1.5	9.5	0.39	1.14
	5	1.4	9.0	0.47	1.30
9-AS	1	1.6	9.0	0.35	1.23
	2	1.5	8.7	0.43	1.29
	3	1.6	8.4	0.45	1.24
	5	1.3	8.1	0.58	1.61

for the fluorescence decay becomes a simple two-exponential decay:

$$I(t) = c_1 \exp[-t/\tau_1] + c_2 \exp[-t/\tau_2] \quad (7)$$

The analysis with τ_1 fixed at 10.8 ns (EXP2-model) resulted in unacceptable statistical parameters (Table 3). In the EXP3-model both lifetimes were allowed to float. Thus, the exponential terms correspond to the decay of 11-CU molecules contacting a phase of the acceptor layers with a low, $c_1 \exp[-t/\tau_1]$, and a high, $c_2 \exp[-t/\tau_2]$, acceptor concentration. Acceptable statistical parameters were obtained at low acceptor concentrations. However, the analysis is not successful at acceptor concentrations exceeding 3 mol %.

2DF Model, Submodel 2. In the other limit of the BF model where the layers are infinitely close, eq 6 transforms into the two-dimensional Förster model (donors and acceptors in the same plane)

$$I(t) = \alpha \exp[(-t/\tau_D) - \gamma_2(t)^{1/3}] + (1-\alpha)\exp[-t/\tau_2] \quad (8)$$

According to Baumann and Fayer,[8] γ_2 becomes $1.1466\sigma_i\pi R_0^2(\tau_D)^{-1/3}$ in the static case. The results from global analysis of the decay curves in the framework of eq 8 with τ_D and τ_2 fixed at 10.8 ns (2DF2 model) are listed in Table 4. At low 9-AS concentrations, satisfactory fits were obtained even without the extra exponentially decaying term (2DF1 model). For 3 and 5 mol % 9-AS and for all 2-AS films the exponentially decaying term should be included in the analysis to obtain acceptable values of the statistical parameters (2DF2 model). The relative contribution of the exponentially decaying term, $1-\alpha$, is high and decreases with increasing acceptor concentration. Again, the obtained γ_2 values increase linearly with increasing acceptor concentration but do not approach zero at low acceptor concentrations.

2DF Model, Submodel 3. The results obtained by global fitting allowing the exponentially decaying term to float (2DF3 model) are also listed in Table 4. The fluorescence lifetimes τ_2 of 1.3 and 1.2 ns for 2-AS and 9-AS, respectively, were obtained. The γ_2 values obtained are clearly smaller than those obtained with the 2DF2 model for both acceptors. For 2-AS the obtained γ_2 values increase linearly with increasing acceptor concentration, but for 9-AS the γ_2 value obtained for the 5 mol % film deviates from linear dependence.

TABLE 4: Parameters Obtained by Global Analysis of the Donor Fluorescence Decay Curves in the Framework of Förster Energy Transfer in Two-Dimensional System with (2DF2 and 2DF3) and without (2DF1) the Extra Exponentially Decaying Term[a]

	[*i*-AS]	2-AS			9-AS		
model	(mol %)	γ_2	$1-\alpha$	χ^2	γ_2	$1-\alpha$	χ^2
2DF1	1	0.24		2.22	0.37		1.12
	2	0.30		2.72	0.46		1.18
	3	0.35		2.91	0.56		1.47
	5	0.47		3.03	0.62		2.07
	global χ^2			2.32			1.40
2DF2	1	0.92	0.38	1.13	0.69	0.22	1.16
	2	0.95	0.31	1.18	0.75	0.16	1.18
	3	1.01	0.27	1.19	0.94	0.10	1.22
	5	1.12	0.18	1.03	1.00	0.11	1.22
	global χ^2			1.14			1.19
2DF3	1	0.15	0.20	1.19	0.31	0.13	1.18
	2	0.19	0.23	1.11	0.38	0.14	1.16
	3	0.22	0.25	1.13	0.47	0.14	1.16
	5	0.30	0.28	1.14	0.48	0.21	1.17
	global χ^2			1.14			1.17

[a] τ_D is fixed at 10.8 ns. For 2DF3 the lifetime of the exponential term was 1.3 ± 0.2 ns and 1.2 ± 0.2 ns for 2-AS and 9-AS, respectively.

TABLE 5: Parameters Obtained by Global Analysis of the Donor Fluorescence Decay Curves in the Framework of Stretched Exponential Equation with (SE2) and without (SE1) the Extra Exponentially Decaying Component[a]

	[*i*-AS]	2-AS				9-AS			
model	(mol %)	$\gamma_{\bar{d}}$	$\bar{d}$	$1-\alpha$	χ^2	$\gamma_{\bar{d}}$	$\bar{d}$	$1-\alpha$	χ^2
SE1	1	0.90	0.72		1.12	0.72	1.22		1.10
	2	1.11	0.72		1.12	0.89	1.22		1.16
	3	1.27	0.72		1.10	0.99	1.22		1.19
	5	1.69	0.72		1.12	1.20	1.22		1.13
	global χ^2				1.12				1.18
SE2	1	0.76	2.74	0.47	1.17	0.64	2.35	0.27	1.16
	2	0.78	2.74	0.40	1.18	0.69	2.35	0.21	1.16
	3	0.82	2.74	0.35	1.18	0.84	2.35	0.14	1.12
	5	0.89	2.74	0.26	1.10	0.89	2.35	0.14	1.12
	global χ^2				1.16				1.14

[a] τ_D is fixed at 10.8 ns.

SE Model. A different approach by Klafter and Blumen[9] led to an expression for the fluorescence decay similar to the 2DF model, but in which the fractal dimension of the system ($\bar{d}$) is allowed to vary

$$I(t) = \alpha \exp[(-t/\tau_D) - \gamma_{\bar{d}}(t)^{\bar{d}/6}] + (1-\alpha)\exp[-t/\tau_2] \quad (9)$$

where the parameter $\gamma_{\bar{d}}$ still depends on the critical transfer distance, R_0, and the number of acceptors in a unit area, σ_i. The fractal dimension $\bar{d}$ would suggest fractal-like structures in the monolayers, leading to a self-similar distribution of acceptors around the donor molecules. This distribution must be self-similar on a nanometer scale typical for Förster transfer. Global analysis in the framework of eq 9, without the extra exponentially decaying term (SE1), τ_D fixed at 10.8 ns, and linking the parameter $\bar{d}$ resulted in acceptable statistical fits (Table 5) with $\bar{d}$ values of 0.72 ± 0.21 and 1.22 ± 0.18 for 2-AS and 9-AS, respectively. The quality of the fit was the same with $\bar{d}$ fixed at 1.

Since the statistics are good for the SE model without the extra exponentially decaying term, no improvement fitting the full expression of eq 9 is expected. However, allowing the extra exponentially decaying term to be present might help to restore the physical meaning of the parameters. Global analysis

including an exponentially decaying term fixed at $\tau_2 = 10.8$ ns (SE2) resulted in $\bar{d}$ values of 2.7 ± 0.6 and 2.4 ± 0.5 for 2-AS and 9-AS, respectively (Table 5). The quality of the fits was nearly same with $\bar{d}$ fixed at 2 (2DF model) or $\bar{d}$ fixed at 3. The obtained $\gamma_{\bar{d}}$ values increase linearly with increasing acceptor concentration with small differences in the slopes but again do not approach zero at low acceptor concentration.

Acceptor Fluorescence. The fluorescence spectra of 2-AS and 9-AS with different concentrations are shown in Figure 8. With increasing 2-AS concentration the fluorescence maximum shifts to the red, whereas for 9-AS the red shift is observed only at low concentrations from 1 to 5 mol %, and the spectrum of the 100 mol % film is blue-shifted relative to the diluted ones. For 2-AS the changes in the spectra could be explained by aggregation, but for 9-AS this leads to the paradox that 100 mol % film would be the least aggregated. The changes in the fluorescence spectra also suggest that the mixed films do not undergo a complete phase separation of the probe and matrix molecules, forming patches of undiluted 2-AS and 9-AS. If this would be the case, the fluorescence spectra of 100 mol % and diluted films should be identical.

Because of the position where the acceptor is incorporated in the films, 9-AS experiences a hydrophobic environment and 2-AS experiences a hydrophilic environment. Thus, the changes observed in the fluorescence maxima with increasing concentration could be due to changes in the local polarity experienced by the chromophores.[6,32−34] With increasing polarity a red shift of the fluorescence spectrum is expected. This would suggest that in the 100 mol % film the anthroyloxy groups of 2-AS are squeezed out of the alkane part of the layer, whereas for 9-AS the anthroyloxy groups stay in the alkane part of the film. This is in agreement with the different pressure−area isotherms observed for the 100 mol % films.

The fluorescence decay curves of 1 mol % 2-AS and 9-AS in the absence of 11-CU, excited at 295 nm and monitored at 450 nm, can be fitted to a two-exponential decay with lifetimes of 1.6 ± 0.4 and 10.6 ± 0.1 ns. This is in good agreement with previous studies of 2-AS in stearic acid LB films.[35] In dilute solutions one-exponential decays with a lifetime of 8.3 ± 0.1 ns are observed. In LB films the chromophores are characterized by a reduced orientational freedom and aggregation is frequently encountered.[4,5,36] If both monomers and aggregates of acceptors, i.e., low and high concentration phases, are present in the films, both species can act as a primary acceptor, and in a second step the monomers will transfer the energy further to aggregates. Upon increasing the acceptor concentration the monomer−aggregate ratio is not expected to change significantly over the concentration range used, since the excitation spectra of the acceptors are independent of concentration and monitoring wavelength. The proportion of the long-lived component is 0.22 and 0.50 for 2-AS and 9-AS, respectively. This indicates a different solubility in the different phases for 2-AS and 9-AS. The acceptor decay curves monitored at 450 nm in the presence of 11-CU are one-exponential with a lifetime of 10.6 ± 0.1 ns. Because of limitations in the possible excitation wavelengths in our measuring system, exciting only the acceptor molecules in the composite films was not possible. The fluorescence intensity of acceptors in the absence of donors with the excitation wavelength of 295 nm is very weak, but in the presence of donors the intensity is more than 10 times higher (Figure 5). Thus, the observed one-exponential decays are due to selective, indirect excitation of acceptors.

4. Discussion

11-CU is one of the few compounds giving a single-exponential decay in LB films.[37,38] For other chromophores in other multilayer systems even at very low chromophore concentrations of 0.2 mol %, clearly nonexponential fluorescence decays are observed[4,39,40] due to inhomogeneous distribution of the molecules in the films. For the present system assuming a random distribution of the donor molecules in the monolayer, the average distance between 11-CU molecules in the present films is estimated from the mean molecular area at the deposition pressure to be $(0.01 \times 19.6\ \text{Å}^2)^{1/2} = 44$ Å for 1 mol % concentration. The minimum distance between 11-CU molecules in adjacent layers is 40 Å for 9-AS films and 50 Å for 2-AS films. These values are significantly larger than the critical transfer distance of energy migration among donors,[24] $R_0 = 21$ Å. Thus, the energy migration between donor molecules can be neglected under the present conditions.

The minimum distances between 11-CU and the anthroyloxy molecules in different layers are depicted in Figure 2. For 9-AS only the closest acceptor layer, $d = 17.5$ Å, is close enough for energy transfer, whereas for 2-AS besides the closest layer, $d = 20$ Å, also the second closest, $d = 30$ Å, can have a small influence on the energy transfer kinetics.

According to previous studies,[41,42] 11-CU in fatty acid matrix LB film is oriented with its chromophore long and short axes at an average of 35° with respect to the substrate surface. This orientation can differ slightly with the deposition conditions such as surface pressure, subphase, and matrix compound. Since the 9-anthroyloxy S_1 transition dipole is oriented with the short axis of the chromophore moiety in the layer plane,[43] the reduced orientational freedom in LB films does not decrease the efficiency of energy transfer compared with isotropic solution.

The submodels BF1, SE1, and 2DF1 assuming a homogeneous distribution of acceptors clearly fail in all cases. The BF1 model (eq 2) should be an adequate model to simulate the physical properties of the present films. However, using the predetermined parameters, the model does not fit the experimental decays. The efficiency for energy transfer, E_{ET}, can be calculated as $1 - I/I_0$, where I is the area found by numerical integration of the decays simulated by the BF expression (eq 2) in the presence of acceptors and I_0 is the corresponding area of the exponential decay of the donor in the absence of acceptors. Because the layer separation in our systems is significantly smaller than R_0, E_{ET} is expected to approach 85% at 5 mol % acceptor concentration. This is not observed in the donor decay curves, as judged from the comparison of measured and simulated data (Figure 7).

In the literature[1,3,5,6,40] fluorescence decay curves of interlayer energy transfer systems in LB films are often analyzed as stretched exponentials (SE model), allowing the fractal dimension parameter to float and vary between different decays. The analysis of the present decay curves in the framework of eq 9 without the extra exponential component yielded (SE1) a fractal dimension of $\bar{d} \approx 1$ for both acceptors and all concentrations. In previous studies[1,3,5,6] of LB films containing chromophores the values of $\bar{d}$ have been found to vary with the acceptor concentration. For monolayer films values smaller than 2 have been found for $\bar{d}$, whereas for multilayer films $\bar{d}$ increases upon increasing number of layers. The small values of $\bar{d}$ found by other authors[1,3,5,6] for monolayer films have been explained by an irregular distribution of the chromophores in the films. The increase of $\bar{d}$ upon increasing the number of successive layers for a multilayer system[3] was explained by energy transfer occurring between chromophores embedded in nonadjacent

layers. Thus, the decay law for energy transfer in a two-dimensional system cannot be applied to stacked multilayer systems when the interlayer distance is not much larger than R_0. For a double-alternating system of acceptors and donors, where energy transfer to acceptor layers on both sides of the donor layers was possible, the two-dimensional system has been found to approach the three-dimensional one with increasing acceptor concentration.[40] For the present films the quality of the fit was the same fixing $\bar{d}$ to 1 without or 2 and 3 with the extra exponentially decaying term.

In the submodels BF2, EXP2, 2DF2, and SE2 it is assumed that the acceptor layer consists of two phases: one containing only SA and the other containing SA and acceptor molecules. Thus, an additional exponentially decaying term due to donor molecules unaffected by any acceptors was included. The lifetime of this component was fixed at 10.8 ns, i.e., the lifetime of donor molecules in LB films without any acceptors. Models BF2, 2DF2, and SE2 gave acceptable statistical results, whereas model EXP2 clearly failed. For these models, which assume that an important amount of donors is not quenched by energy transfer, the analysis of the fluorescence decays should yield a significant value of the factor $1 - \alpha$. Indeed, the obtained $1 - \alpha$ values are fairly high, increasing with decreasing acceptor concentration for all cases. At low acceptor concentration unexpectedly high γ values are obtained with all three models. Clearly extrapolating to $\gamma \rightarrow 0$ for $\sigma_{tot} \rightarrow 0$ cannot be done. These large γ values suggest the presence of domains with high local acceptor concentration, leading to a relatively efficient energy transfer already at low acceptor concentrations. This kind of acceptor distribution is modeled with submodels 3.

Global analysis of the decay curves with SE2 model gave fractal dimensions of 2.7 for 2-AS and 2.4 for 9-AS. These values are relevant as in the present systems the energy transfer takes place from one plane to another. Thus, the dimensionality is restricted in one direction ($\Rightarrow \bar{d} < 3$), but the donor and acceptor planes are not infinitely close ($\Rightarrow \bar{d} > 2$). The higher dimensionality obtained for the 2-AS system can be due to the possibility of energy transfer to more than one acceptor layer (Figure 2).

In the submodels BF3, EXP3, and 2DF3 it is assumed that the acceptor layers have two phases: one of low acceptor concentration and the other of high acceptor concentration. Thus, the lifetime of the exponential component was allowed to float, yielding the inverse rate of the energy transfer occurring at the phase with high acceptor concentration. Acceptable statistical parameters were obtained with models BF3 and 2DF3.

The fluorescence lifetimes obtained for the exponentially decaying terms were nearly equal for models BF3 and 2DF3. Furthermore, $1 - \alpha$ increases with increasing acceptor concentration. This is opposite to our observations for BF2 and 2DF2. In the models BF2 and 2DF2 the term $1 - \alpha$ corresponds to the exponential component representing donors that are not contacting a phase containing acceptors. Hence, the importance of this component should decrease upon increasing the overall surface density of acceptors. On the other hand, in the models BF3 and 2DF3 the term $1 - \alpha$ corresponds to the fast decaying component representing donors that are contacting a phase saturated with acceptors. Hence, it can be expected that the proportion of this component increases upon increasing the overall surface density of acceptors, indicating that the high-concentration phase becomes more important upon increasing the overall acceptor concentration. The absolute values of $1 - \alpha$ are relatively high. If the high-concentration phase of the acceptors would contain only acceptor molecules, $1 - \alpha$ at 5 mol % should not be higher than 0.05 and 0.10 for 9-AS and 2-AS, respectively. The high $1 - \alpha$ values can be due to parameter correlation, which would also explain the deviation from linear dependence of γ_{IL} observed for 5 mol % 9-AS. On the other hand, the same effect would be observed if the high-concentration phase is also diluted by the matrix molecules, increasing the area of the phase by a factor of 3−13 (Table S1).

TABLE 6: Acceptor Concentrations σ_i for the High and Low Acceptor Concentation Phases Calculated from the Results Obtained by the BF3 Model with R_0/d Fixed

[*i*-AS] (mol %)	σ_{tot} (nm^{-2})	σ_{low} (nm^{-2})	$[i\text{-AS}]_{low}$ (mol %)	σ_{high} (nm^{-2})	$[i\text{-AS}]_{high}$ (mol %)
9-AS					
1	0.051	0.025	0.5	0.162	3
2	0.100	0.032	0.6	0.341	7
3	0.148	0.039	0.8	0.493	11
5	0.240	0.039	0.8	0.667	15
2-AS, $b = 0.5$					
1	0.051	0.0126	0.2	0.166	3
2	0.100	0.0162	0.3	0.305	6
3	0.148	0.0179	0.4	0.424	9
5	0.240	0.0251	0.5	0.576	13
2-AS, $b = 1.0$					
1	0.051	0.0063	0.1	0.185	4
2	0.100	0.0081	0.2	0.325	7
3	0.148	0.0090	0.2	0.443	10
5	0.240	0.0126	0.2	0.600	13

The γ values obtained with models BF3 and 2DF3 are much lower than those obtained with models BF2 and 2DF2, since in the submodels 3 the major part of the energy transfer is described by the extra term. This results in smaller γ values extrapolating to $\sigma_{tot} \rightarrow 0$ for submodels 3 (Figure 8). From the parameters γ_{IL}, τ_D, and R_0 obtained with the model BF3, the number density of the acceptors in the low acceptor concentration phase can be calculated. Assuming that the acceptor molecules in this phase exist as monomers, the R_0 value of 28 Å calculated from the solution data was used. For 9-AS only the closest acceptor layer with $d = 17.5$ Å is close enough for energy transfer. Thus, the parameter b in the relation of γ_{IL} is equal to 0.5. For 2-AS besides the closest layer with $d = 20$ Å also the second closest layer with $d = 30$ Å can take part in the energy transfer. Thus, the acceptor concentrations were calculated using both b values 0.5 and 1. The results are listed in Table 6. Knowing the average number density of the acceptor molecules and the number density in the low-concentration phase, the acceptor number density in the high-concentration phase can be estimated with the simple relation $\sigma_{tot} = \alpha\sigma_{low} + (1 - \alpha)\sigma_{high}$, where α and $(1 - \alpha)$ are the fractions of the two terms of the decay function. The results together with the estimated concentrations in mole percent are listed in Table 6. Both concentrations increase with increasing acceptor concentrations, but the increase is larger for the high concentration phase. The results for 2-AS using b values 0.5 and 1 are nearly equal. The γ_{IL} and $1 - \alpha$ values used to calculate the results for 2-AS in Table 6 were obtained by fixing R_0/d at 1.4. Nearly equal results are obtained using γ_{IL} and $1 - \alpha$ values obtained by fixing R_0/d at 1.1 ($d = 25$ Å) or 0.9 ($d = 30$ Å).

The energy transfer is clearly more efficient for 9-AS than for 2-AS as probed by steady-state and time-resolved measurements. The perpendicular distance between the donors and acceptors is 17.5 Å for 9-AS and 20 or 30 Å for 2-AS. Because of the d^{-4} relationship between the distance and the efficiency of the energy transfer,[44,45] the acceptor layer at $d = 20$ Å has an efficiency of 58% of a layer with $d = 17.5$ Å. The layer at $d = 30$ Å has an efficiency of 11% of a layer with $d = 17.5$ Å. Thus, both 2-AS layers together have an efficiency of 70% of the one 9-AS layer at $d = 17.5$ Å.

The proportion of the short-lived component in the fluorescence decay curves of acceptors in the absence of donors is higher for 2-AS than for 9-AS, suggesting a higher degree of aggregation for 2-AS. The same is observed in the presence of donors: $1 - \alpha$ is higher for 2-AS than for 9-AS. Thus, the high-concentration phase seems to occupy a larger fraction of the monolayer for 2-AS than 9-AS. This could be due to the different environment experienced by the two acceptors in the films. The acceptor concentration in the high concentration phase seems to be nearly equal for both acceptors.

5. Conclusions

In the present study, the interlayer excitation energy transfer between 11-CU and 9-AS and 2-AS in LB films was examined with picosecond time-resolved fluorescence decay measurements. Four models were used to analyze the decay curves. The failure of the simulations with the BF1 model suggested an inhomogeneous distribution of acceptor molecules in the films. Formation of two separate phases is suggested: one of low acceptor concentration and another of high acceptor concentration. The fluorescence quenching of the donor molecules facing the low acceptor concentration phase follows the BF model for interlayer energy transfer. An extra exponential component due to the donor molecules quenched by the high acceptor concentration phase was included in the analysis. In the literature the fluorescence decay curves for systems with donors and acceptors in different layers could be analyzed with acceptable statistical fits as a stretched-exponential decay only when the fractal dimension parameter was allowed to float. Using the model for interlayer energy transfer proposed by Baumann and Fayer (BF model), it is not necessary to allow the dimension to float to obtain satisfactory fits for the present Langmuir−Blodgett films. These are the first results where two-dimensional interlayer energy transfer in Langmuir−Blodgett films analyzed by the BF model yielded successful fitting and meaningful decay parameters.

Acknowledgment. K.K.J. is grateful to the Nordic Network on Polarization Spectroscopy supported by NorFA for financial support and to the Danish Research Academy for a fellowship. B.A. gratefully acknowledges support from the Swedish Natural Science Research Council (NFR) and the Swedish Research Council for Engineering Sciences (TFR). M.V.d.A. is an "Onderzoeksdirecteur" of the F.W.O.-Vlaanderen (Fonds voor Wetenschappelijk Onderzoek Vlaanderen) and thanks the "Nationale Loterij", the F.W.O.-Vlaanderen, and D.W.T.C. through IUAP IV-11. E.V. and H.L. gratefully acknowledge the financial support of the Academy of Finland and the Technology Development Center of Finland for support of our program of photochemistry of organic films.

Supporting Information Available: Maximum surface densities of the high-concentration phase. This material is available free of charge via the Internet at http://pubs.acs.org.

References and Notes

(1) Yamazaki, I.; Tamai, N.; Yamazaki, T. *J. Phys. Chem.* **1990**, *94*, 516.
(2) Tamai, N.; Matsuo, H.; Yamazaki, T.; Yamazaki, I. *J. Phys. Chem.* **1992**, *96*, 6550.
(3) Ohta, N.; Tamai, N.; Kuroda, T.; Yamazaki, T.; Nishimura, Y.; Yamazaki, I. *Chem. Phys.* **1993**, *177*, 591.
(4) Ballet, P.; Van der Auweraer, M.; De Schryver, F. C.; Lemmetyinen, H.; Vuorimaa, E. *J. Phys. Chem.* **1996**, *100*, 13701.
(5) Vuorimaa, E.; Belovolova, L. V.; Lemmetyinen, H. *J. Lumin.* **1997**, *71*, 57.
(6) Tamai, N.; Yamazaki, T.; Yamazaki, I. *Can. J. Phys.* **1990**, *68*, 1013.
(7) Caruso, F.; Thistlewaite, P. J.; Grieser, F.; Furlong, D. N. *Langmuir* **1994**, *10*, 3373.
(8) Baumann, J.; Fayer, M. D. *J. Chem. Phys.* **1986**, *85*, 4087.
(9) Klafter, J.; Blumen, A. *J. Chem. Phys.* **1984**, *80*, 875.
(10) The thickness of a double and a single layer of SA is known from the literature (Roberts, G. *Langmuir−Blodgett Films*; Plenum Press: New York, 1990; pp 26−27). Furthermore, the small amount of the chromophores (up to 5 mol %) is assumed not to disturb this parameter. Also, the hydrocarbon chains of 11-CU, 9-AS, and 2-AS in the films are assumed to be stretched. This is often done for LB films (Roberts, G. *Langmuir−Blodgett Films*; Plenum Press: New York, 1990 and references therein). Thus, on the basis of these assumptions, the center-to-center distances between the chromophore parts of the modified fatty acids were estimated with a HyperChem program.
(11) Marquardt, D. W. *J. Soc. Ind. Appl. Math.* **1963**, *11*, 431.
(12) Knutson J. R.; Beechem J. M.; Brand, L. *Chem. Phys. Lett.* **1983,** *102*, 501.
(13) Eisenfeld, J. In *Time-Resolved Fluorescence Spectroscopy in Biochemistry and Biology*; Cundall, R. B., Dale, R. E., Eds.; Plenum Press: New York; 1983; p 233.
(14) Caterall, In *Time-Resolved Spectroscopy in Biochemistry and Biology*; Cundall, R. B., Dale, R. E., Eds.; Plenum Press: New York, 1983.
(15) Durbin, J.; Watson, G. S. *Biometrika* **1950**, *37*, 409; **1951**, *38*, 159; **1971**, *58*, 1.
(16) Grinvald, A.; Steinberg, I. Z. *Anal. Biochem.* **1974**, *59*, 583.
(17) Boens, N.; Van den Zegel, M.; De Schryver, F. C. *Chem. Phys.* **1988**, *121*, 73.
(18) Van den Zegel, M.; Szabo, A. G.; Bramall, L.; Krajcarski, D. T.; Selinger, B. *Rev. Sci. Instrum.* **1985**, *56*, 14.
(19) Lentz, B. R. *Spectroscopic Membrane Probes*; Loew, L. M., Ed.; CRC Press: Boca Raton, FL, 1988; Vol. 1, pp 13−41.
(20) (a) Förster, T. *Naturwissenschaften* **1949**, *33*, 166. (b) Förster, T. *Ann. Phys.* **1948**, *2*, 55.
(21) *Handbook of Chemistry and Physics*, 75th ed.; Lide, D. R., Ed.; CRC Press: Boca Raton, FL, 1995.
(22) Lakowicz, J. R. *Principles of Fluorescence Spectroscopy*; Plenum Press: New York, 1983; pp 303−309.
(23) Guilbault, G. *Practical Fluorescence*; Marcel Dekker: New York, 1976.
(24) Berlman, I. B. *Energy Transfer Parameters of Aromatic Compounds*; Academic Press: New York, 1973.
(25) Tamai, N.; Yamazaki, T.; Yamazaki, I. *J. Phys. Chem.* **1987**, *91*, 841.
(26) Robert, S.; Tancrede, P.; Salesse, C.; Leblanc, R. C. *Biochim. Biophys. Acta* **1983**, *730*, 217.
(27) Srinivasan, M. P.; Lau, K. K. S. *Thin Solid Films* **1997**, *307*, 266.
(28) Vuorimaa, E.; Lemmetyinen, H.; Van der Auweraer, M.; De Schryver, F. C. *Thin Solid Films* **1995**, *268*, 114.
(29) Cadenhead, D. A.; Kellner, B. M. J.; Jacobson, K.; Papahadjopoulos, D. *Biochemistry* **1977**, *16*, 5386.
(30) Verschuere, B.; Van der Auweraer, M.; De Schryver, F. C. *Chem. Phys.* **1991**, *149*, 385.
(31) Verschuere, B.; Van der Auweraer, M.; De Schryver, F. C. *Thin Solid Films* **1994**, *244*, 995.
(32) Kemnitz, K.; Murao, T.; Yamazaki, I.; Nakashima, N.; Yoshihara, K. *Chem. Phys. Lett.* **1983**, *159*, 337.
(33) Kemnitz, K.; Tamai, N.; Yamazaki, I.; Nakashima, N.; Yoshihara, K. *J. Chem. Phys.* **1986,** *90*, 5094.
(34) Van der Auweraer, M.; Verschuere, B.; De Schryver F. C. *Langmuir* **1988,** *4*, 583.
(35) Vuorimaa, E.; Ikonen, M.; Lemmetyinen, H. *Thin Solid Films* **1992**, *214*, 243.
(36) Tkachenko, N. V.; Tauber, A. Y.; Lemmetyinen, H.; Hynninen, P. H. *Thin Solid Films* **1996**, *280*, 244.
(37) Gust, D.; Moore, T. A.; Moore, A. L. Luttrull, D. K.; DeGraziano, J. M.; Van der Auweraer, M.; De Schryver, F. C. *Langmuir* **1991**, *7*, 1483.
(38) Yamazaki, I.; Tamai, N.; Yamazaki, T. *J. Phys. Chem.* **1987**, *91*, 3572.
(39) Ballet, P. Ph.D. Thesis, K. U. Leuven, Leuven, 1995.
(40) Vuorimaa, E.; Lemmetyinen, H.; Ballet, P.; Van der Auweraer, M.; De Schryver, F. C. *Langmuir* **1997**, *13*, 3009.
(41) Ohta, N.; Okazaki, S.; Yoshinari, S.; Yamazaki, I. *Thin Solid Films* **1995**, *258*, 305.
(42) Nagamura, T.; Kamata, S.; Ogawa, T. *Ber. Bunsen-Ges. Phys. Chem.* **1992**, *96*, 74.
(43) Matsuki, K.; Fukutome, H. *Bull. Chem. Soc. Jpn.* **1983**, *56*, 1006.
(44) Noukakis, D.; Van der Auweraer, M.; De Schryver, F. C. *J. Phys. Chem.* **1994,** *98*, 11745.
(45) Kuhn, H.; Möbius, D.; Bücher, H. In *Physical Methods of Chemistry, Part 3B*; Weissberger, A., Rossiter, B., Eds.; Wiley: New York, 1972; pp 600−605.